Intelligent Nighttime Video Surveillance Using Multi-Intensity Infrared Illuminator

Peggy Joy Lu, Jen-Hui Chuang, and Horng-Horng Lin

***Abstract*—In nighttime video surveillance, the image details of far objects are often hard to be identified due to poor illumination conditions while the image regions of near objects may be whitened due to overexposure. To alleviate the two problems simultaneously for nighttime video surveillance, we adopt a new multi-intensity infrared illuminator as a supportive light source to provide multiple illumination levels periodically. By using the illuminator with multiple degrees of illumination power, both far and near objects can be clearly captured. For automatic detection of foreground objects at different distances in the image sequences captured with the multi-intensity infrared illuminator, two foreground object detection methods are proposed in this paper. Experimental results show that the two methods both achieve >90% accuracy in average in foreground object detection while giving different computational complexities.**

***Index Terms*—Multi-intensity infrared illuminator, foreground object detection, nighttime video surveillance**

I. Introduction

While nighttime video surveillance plays an important role in crime investigation and prevention, nighttime videos are often complained for low quality due to poor lighting conditions. For example, invaders at far distances from a camera are usually hard to be identified due to limited power of an infrared illuminator (IR-illuminator). On the other hand, human faces close to a camera may become unclear due to image overexposure induced by the strong light from an IR-illuminator. It is quite difficult to find balanced settings for general IR-illuminators to obtain good image qualities for all objects at different distances.

To help solving the problems of underexposure and overexposure simultaneously in nighttime video surveillance, a new *multi-intensity IR-illuminator* that can periodically emit different degrees of power of infrared light [1] is adopted in this work as a supportive light source in video capturing. As shown in Fig.1, the illumination intensities emitted by the adopted IR-illuminator decays exponentially from the brightest level to the darkest one in each period, which has been demonstrated to be an effective design in [1] for reducing blurred imaging results. With the multi-intensity IR-illuminator, foreground object at distances can be clearly observed in the images of high illumination levels while near objects can be properly captured in those of low illumination levels.

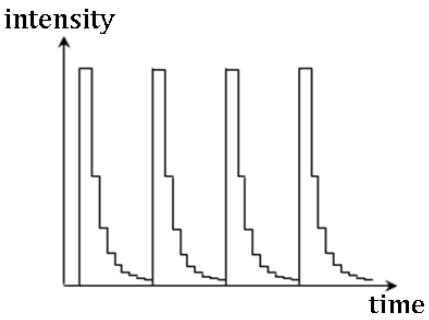

Fig. 1. Periodic changes of the illumination intensities of the multi-intensity IR-illuminator.

Despite the stable changes of the emitted illumination intensities by the multi-intensity IR-illuminator, the observed changes of image intensities in the captured video sequences could vary largely. For example, an image sequence of a white wall captured with the multi-intensity IR-illuminator is shown in Fig. 2, wherein two periods of illumination changes from bright to dark are included. One can observe in Fig. 2 that the number of image frames in each *illumination period* is not a constant because the timing of illumination changes of the IR-illuminator and that of camera shutter controls are not synchronized. Therefore, the correct identification of each illumination period should be the first task for the analysis of such a video sequence.

Based on the characteristic of a sudden increase of illumination intensity from the lowest level to the highest level between two periods, as shown in Fig. 1, one can easily segment each illumination period in a video sequence by checking if there is a large increase of the average image intensity between two neighboring frames. Here we apply simple thresholding of the intensity difference between two consecutive frames to segment each illumination period. Note that, due to the asynchronous timing controls between the multi-intensity IR-illuminator and the camera shutter, transitional image frames, one example of which shown in Fig. 2, may be found on the adjacency of two illumination periods. These transitional image frames will be discarded from further analysis.

Once the illumination periods being identified, we further group the images that are captured at a similar illumination

Manuscript received Jul. 15, 2011; revised Aug. 16, 2011. This work is supported in part by 99-EC-17-A-02-S1-032, NSC 100-2220-E-009-057, NSC 100-2220-E-009-052 and "Aim for the Top University Plan" of National Chiao Tung University and Ministry of Education, Taiwan.

Peggy Joy Lu is with the Department of Computer Science, National Chiao Tung University, Taiwan. (e-mail: superorange.cs98g@nctu.edu.tw).

Jen-Hui Chuang is with the Department of Computer Science, National Chiao Tung University, Taiwan. (e-mail: jchuang@cs.nctu.edu.tw).

Horng-Horng Lin is with the Department of Computer Science and Information Engineering, Southern Taiwan University, Taiwan. This work was done while he was with the Computer Vision Research Center, National Chiao Tung University, Taiwan. (phone: +886-3-5712121#56635; e-mail: hhlin.tw@gmail.com).

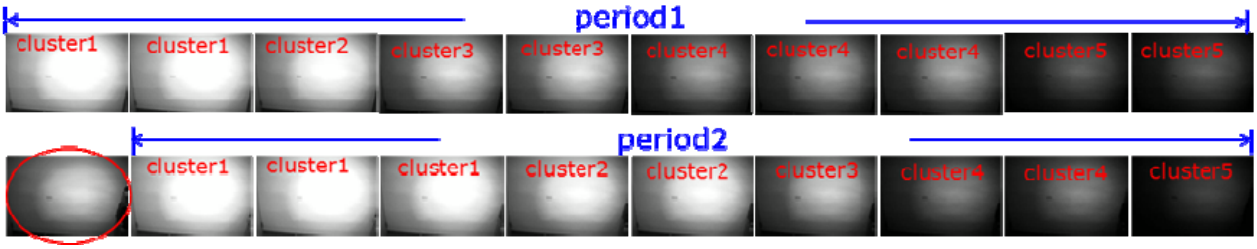

Fig. 2. An image sequence containing two illumination periods captured with the multi-intensity IR-illuminator. Five *illumination clusters* can be identified in each period. The circled frame is a transitional image between the sudden illumination changes from the darkest level to the brightest level.

level across different illumination periods into an *illumination cluster*. Each illumination cluster can be regarded as an independent video sequence captured with a constant-level IR-illuminator and as a basic processing unit for foreground object analysis. The details of illumination clustering will be described later in Sec. II-B.

A. The Proposed Methods

Two methods, (i) *background modeling based on illumination clustering* and (ii) *periodic min-max modeling*, are proposed for foreground object detection in video sequences captured with the multi-intensity IR-illuminator. In Method (i), we first apply *illumination clustering* to classify image frames across different periods into illumination clusters of similar illumination levels. Then we use background subtraction to extract foreground objects in each illumination cluster. For Method (ii), a novel *periodic min-max modeling* approach that gives similar accuracy in foreground object detection to the Method (i) with more efficiency is proposed. The Method (ii), while still rooted in the concept of background subtraction, requires less computation of background models in the extraction of foreground objects.

B. Related Work

To solve both the problems of underexposure and overexposure in image capturing, the idea of employing more than two exposure settings is adopted by several research studies. For example, [2] and [3] acquire high dynamic range images with different exposure settings and perform image synthesis for better visualization. Mangiat and Gibson [4] take videos by two cameras with two exposure settings for further video enhancement. In contrast to these studies that apply multiple exposure settings in video capturing, we instead apply a new multi-intensity IR-illuminator as a supportive light source in nighttime video acquirement.

Regarding human detection in nighttime videos, Benezeth *et al.* [5] use a far infrared camera to take images under low-light conditions and apply Gaussian mixture modeling to human object extraction. Nevertheless, far infrared cameras are much more expensive than near infrared ones, resulting in less popularity in nighttime surveillance.

Instead of using background subtraction for foreground object extraction, many researches adopt machine learning techniques to detect human in nighttime videos. For example, both the driver-assistance systems developed by Ge *et al.* [6] and Fang *et al.* [7] use image segmentation and pedestrian shape learning to detect human. Similarly, Bertozzi *et al.* [8] and Dai *et al.* [9] apply human shape learning to the identification of human objects by using stereo and monocular camera, respectively. In [10], Xu *et al.* use support vector machines to learn head and body shapes for solving occlusion problems. Nanda and Davis [11] used probability template to identify human objects in occlusions and under low contrast conditions.

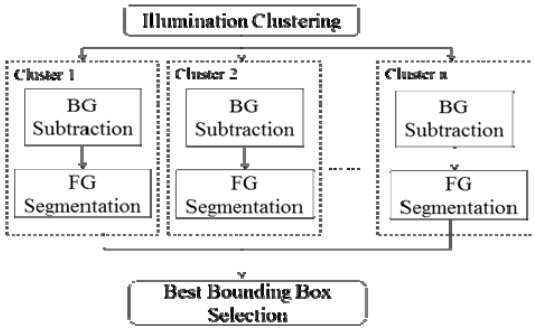

Fig. 3. The flowchart of background modeling based on illumination clustering.

II. Background Modeling Based on Illumination Clustering

The flowchart of the Method (i), *background modeling based on illumination clustering*, is illustrated in Fig. 3. Given an image sequence captured with a multi-intensity IR-illuminator, we classify the video frames into N illumination clusters. Each illumination cluster consists of selected images captured at a similar illumination level. A single Gaussian background model is then constructed for each illumination cluster and the background subtraction is performed to extract foreground objects from the clustered images. The extracted foreground objects will be further identified as human and non-human by checking the size ratios of object bounding boxes and gradient distributions. Finally, human objects with clear gradients will be selected for visual display.

A. Representative Blocks

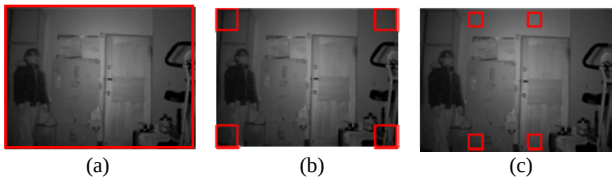

(a) (b) (c)

Fig. 4. Three choices of representative blocks for illumination clustering.

Prior to the illumination clustering, we need to specify image regions to determine the illumination level of an image frame. In Fig. 4, three choices of *representative blocks* for the determination of image illumination levels are presented. In Fig. 4(a), the intensity mean of the whole image is used for

ISBN: 978-988-18210-9-6
ISSN: 2078-0958 (Print); ISSN: 2078-0966 (Online)

the estimation of illumination level. However, the estimation of illumination level based on this choice will be affected by foreground objects passing by the scene. Because foreground objects often appear in the central region, one may consider corner blocks of an image (Fig. 4(b)) as representatives for the estimation of the illumination level of a background scene. Nevertheless, due to uneven lighting, the illumination levels of the corner blocks are darker than those of the central area, which will result in under-estimation of the illumination level of an image. We therefore turn to the choice of four surrounding blocks shown in Fig. 4(c) as representatives for illumination level estimation.

B. *Illumination Clustering*

To begin with, we classify the image frames in the first period of illumination change into N standard illumination clusters. Here we assume that no foreground objects appear at the representative blocks in the image frames of the first period. As shown in Fig. 5(a), N=4 clusters can be identified in the first period by performing raster scan of the images of the first period and thresholding the average intensity difference of the representative blocks between each pair of neighboring frames. If the difference between two neighboring frames is larger than a pre-defined threshold, a new illumination cluster is created.

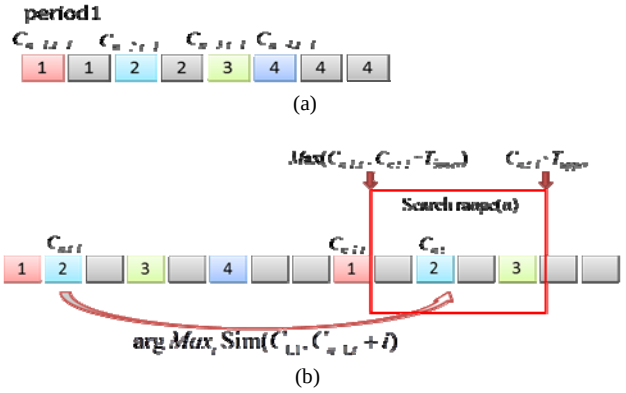

Fig. 5. Search range for illumination clustering (a) N=4 clusters identified in first period. (b) Selection of the corresponding frame to the 2nd cluster in tth period.

Once the N illumination clusters of the first period are obtained, N corresponding frames to the N clusters will be selected in each subsequent period. Specifically, as shown in Fig. 5(b), we find the corresponding frame to the nth (n=2) cluster by searching the image frames within a search range. Since the number of image frames of a period of illumination change varies from T_{lower}=10 to T_{upper}=20 frames, we define the search range from $max(C_{n-1,t}, C_{n,t-1}+T_{lower})$ to $C_{n,t-1}+T_{upper}$, where $C_{n-1,t}$ denotes the frame index of the corresponding frame to the (n-1)th cluster of the tth period, and $C_{n,t-1}$ denotes the index of the corresponding frame to the nth cluster of the last period. All the images within the search range are compared to the standard frame of the nth cluster indexed by $C_{n,t=1}$ by computing their intensity differences in the representative blocks. The image frame with the most similar intensity to the standard frame of the nth cluster will then be selected as a corresponding image to the nth cluster in the current period.

C. *Foreground Object Segmentation*

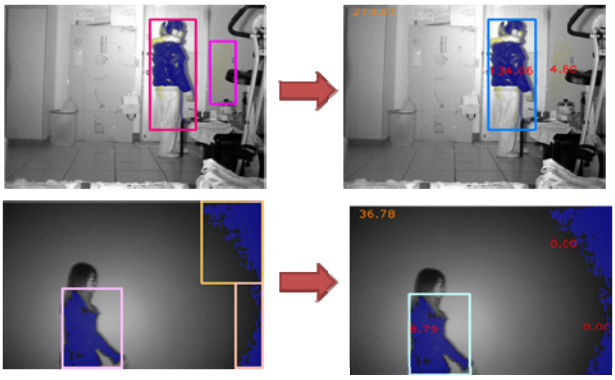

Fig. 6. Erroneous bounding box elimination using gradient information.

The images in each illumination cluster can be regarded as an independent image sequence captured with a constant illuminator. Therefore, the popular single Gaussian background modeling can be used to derive a background model for each cluster. Foreground objects can then be segmented via background subtraction. Here we use the single Gaussian background model instead of Gaussian Mixture Modeling (GMM) for higher computational efficiency. After the background subtraction, the foreground bounding boxes will be computed.

Owing to uneven lighting of the adopted IR-illuminator and the asynchronisms of IR-illuminator and video capturing, some erroneous bounding boxes will be received in foreground object segmentation and need to be filtered out. Since our goal is to detect human, some of the erroneous bounding boxes can be easily eliminated by rejecting improper size ratios and foreground/background pixel ratios. Some other erroneous ones that usually appeared in smooth background area have smaller gradients according to our observations. Thus, we filter out these erroneous bounding boxes by gradient background subtraction, which use gradient to replace intensity in single Gaussian background model. The results after filtering out those wrong bounding boxes are shown in Fig. 6.

D. *Best Bounding Box Selection for Visualization*

Fig. 7. Best bounding box selection by choosing the one with the largest average gradient magnitude among the N clusters.

After obtaining the foreground objects in the N illumination clusters in each illumination period, we can then construct a synthetic image for each period, wherein both the foreground objects and the background scene are clear for human visualization. To identify the clearest foreground object from all the foreground objects in a period, the image gradients of the extracted foreground objects are compared. As shown in Fig. 7, the foreground object with the largest gradient magnitude is chosen as the best one for

ISBN: 978-988-18210-9-6
ISSN: 2078-0958 (Print); ISSN: 2078-0966 (Online)

visualization.

Fig. 8. Best bounding boxes of a person at different distances in different clusters.

The image area of the clearest foreground object will then be merged to the background model with the largest variance among the N background models for the N illumination clusters. Some image synthesis results that show a person walks toward the camera are depicted in Fig. 8. Note that the chosen cluster indices of the clearest foreground objects are changed along with the distance changes of the person to the camera. When the person is at the farthest distance, the best foreground object is chosen from the cluster of highest illumination level. On the contrary, when the person comes close to the camera, the chosen foreground objects are from the clusters of lower illumination levels.

In other words, the best foreground objects are chosen from different illumination clusters according to the distances of the person. The problems of underexposure and overexposure of foreground objects are not observed by using the multi-intensity IR-illuminator with the image synthesis, which demonstrates the effectiveness of the proposed approach. The video quality of nighttime surveillance can thus be significantly improved.

III. Periodic Min-Max Modeling

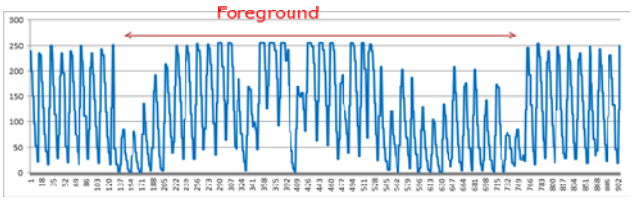

Fig. 9. Periodic illumination variation of one pixel in a video sequence.

Despite the effectiveness of Method (i), *background modeling based on illumination clustering*, for processing the videos captured with the multi-intensity IR-illuminator, the large computational complexity from calculating N background models in Method (i) can be a concern for real-time applications. Therefore, we propose the other method, *periodic min-max modeling,* as a second solution for the analysis of videos captured by the multi-intensity IR-illuminator with lower computational complexity.

Fig. 9 shows the periodic intensity changes of one pixel in a video sequence. Although the intensity levels of the periods of background are not exactly the same, the maximum and the minimum intensity values of the periods of background look quite similar. On the other hand, as the presence of the foreground objects, the maximum and minimum intensity values fluctuate.

Based on the above-mentioned observations, we propose a periodic min-max modeling method wherein two background models are constructed for each pixel to record the periodic changes of the maximum and minimum pixel intensities of a background scene captured with the multi-intensity IR-illuminator. If a pixel is occupied by foreground objects, at least one of its maximum and minimum intensity values will deviate from the corresponding background model so that changes of foreground at this pixel position can be detected. One can clearly see that only two background models need to be maintained in Method (i), resulting in more efficiency than Method (ii) in computation.

In Method (i), background model based on illumination clustering, we use block difference to perform the illumination clustering. However, instead of illumination clustering, Method (ii) only needs to find the cutoff point of each period as the way to get first period in Method (i).

A. Min-Max Background Models

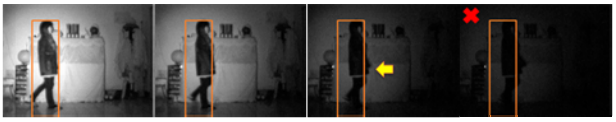

(a)

(b)

Fig. 10. Exclusion of the darkest image. (a) The detected bounding box is not quite correct if the darkest image included. (b) The detected bounding box becomes more accurate after deleting the darkest image.

The way to detect foreground objects in periodic min-max model is similar to common background subtraction approaches based on Gaussian model. In periodic min-max modeling, the minimum and maximum intensities are recorded by two Gaussian models, respectively. Let B_t be an indicator of the foreground label computed by

$$B_t(x,y) = \begin{cases} 1, & if\ |Max_t(x,y) - Max\_\mu_t(x,y)| > \tau \cdot Max\_\sigma_t(x,y) \\ 1, & else\ if\ |min_t(x,y) - min\_\mu_t(x,y)| > \tau \cdot min\_\sigma_t(x,y) \\ 0, & otherwise \end{cases}$$

where (x, y) is the pixel coordinates and $Max_t(x, y)$ is the maximum intensity of the pixel of the period t ; Max_μ_t and Max_σ_t are the mean and the standard deviation, respectively, of the background model for the maximum intensity, and τ=3 is a given threshold. Similarly, the notations of the background model for the minimum intensity can be defined likewise.

For the case of $B_t(x, y) = 0$, it indicates that the pixel is identified as background, and the corresponding Gaussian models need to be updated by

$$Max\_\mu_t(x,y) = (1-\alpha) \cdot Max\_\mu_{t-1}(x,y) + \alpha \cdot Max_t(x,y)$$
$$min\_\mu_t(x,y) = (1-\alpha) \cdot min\_\mu_{t-1}(x,y) + \alpha \cdot min_t(x,y)$$
$$Max\_\sigma_t^2(x,y) = (1-\alpha) \cdot Max\_\sigma_{t-1}^2(x,y) + \alpha \cdot (Max_t(x,y) - Max\_\mu_{t-1}(x,y))^2$$
$$min\_\sigma_t^2(x,y) = (1-\alpha) \cdot min\_\sigma_{t-1}^2(x,y) + \alpha \cdot (min_t(x,y) - min\_\mu_{t-1}(x,y))^2$$

where α is a threshold determined empirically. For the other case of $B_t(x, y) = 1$, we do not update min-max background model because the pixel is identified as foreground, which has great difference with the background. Besides, we also observe that the image intensities of the darkest image in every period are near zero, causing the statistical means of the minimum value meaningless. Thus, as shown in Fig. 10, the darkest image in each period is excluded from the

ISBN: 978-988-18210-9-6
ISSN: 2078-0958 (Print); ISSN: 2078-0966 (Online)

computation of the min-max models.

IV. Experimental Results

The proposed approaches are evaluated by using 14 test video sequences, numbered from 1 to 14. These 14 video sequences are captured at three different scenes. The numbers of image frames of the illumination periods deviate largely in sequences of #1 and #2. The sequences #3 and #4 are blur and of low quality. The sequences of #7 and #8 are captured in outdoor scenes while the sequences of #13 and #14 are captured in different angles of view. In the test video sequences of the gray background videos, #2, #4, #6, #8, #10, #12—#14, contain persons walking toward the cameras and are marked as *vertical videos*. The other video sequences are marked as *horizontal videos* since they contain persons passing by the monitored scenes at fixed distance to the cameras.

We use those 14 different test videos to compute the foreground detection accuracy defined by

$$Accuracy = \frac{TP + TN}{TP + FP + FN + TN},$$

where *TP* and *TN* (*FP* and *FN*) are the true (false) positives and negatives, respectively. The foreground detection accuracies of the 14 test videos using the Method (i) is shown in Table 1. The first part shows the results of all frames while the second part shows the results after the best foreground object selection for better visualization. The accuracies of the horizontal videos are generally higher than those of the vertical videos. In addition, the accuracies increase after the best foreground object selection. Although all the accuracies of all frames in a period are not high due to inappropriate illumination, they are improved after best foreground object selection. Overall, the average accuracy for these 14 test videos is higher than 90%.

The result of periodic min-max model is shown in Table 2. The accuracies both in all frames and in all periods are nearly the same because this method did not use illumination clustering. Since this method use one period as a unit to find one bounding box, an error frame in the period may cause an error result for the whole period. Furthermore, the average accuracy of 14 videos is higher than 90% as well.

V. Conclusion

Table 3. Comparisons of Method (i) and (ii)

	Method (i)	Method (ii)
Illumination clustering	Yes	No
# of background models to be computed	*N*	2
Foreground object detection accuracy	>90%	>90%
Drop of image frames in foreground object detection	Yes	No
Robustness to broken frames	Yes	No

In Table 3, we summerize the comparisons of the Method (i) and (ii). First, the Method (ii) (periodic min-max modeling) does not have to perform the illumination clustering in which some image frames could be excluded from further analysis. More image information can thus be perserved in foreground object detection by the Method (ii) than by the Method (i). Second, the computational complexity of the Method (ii) is lower than that of the Method (i). We note that the Method (i) has to filter out erroneous bounding boxes to achieve higher foreground detection accuracy while the Method (ii) does not need such post-processing. Third, owing to the period-based processing of video frames in the Method (ii), any broken frame in an illumination period caused by large lighting changes will result in a false foreground alert. Instead, the false detection of foreground objects of the Method (i) is less affected by broken frames for its independent processing of N illumination clusters.

In summary, while both the two methods achieve high accuracy (>90%) in foreground object detection, the Method (ii) is recommanded as a more efficient solution to the analysis of video sequences captured with the multi-intensity IR-illuminator for its lower computational complexity. Moreover, the Method (ii) applies all image frames to the analysis of foreground objects while the Method (i) may drop image frames in the illumination clustering and the best bounding box selection. Regarding the future work, possible directions include the enhancement of the robustness to broken frames of the Method (ii) and the extension of the proposed methods to multiple people detection. In addition, integrating the foreground detection methods with the HDR processing for better visualization of detection results could be another interesting research directiosn.

Table 1. Experimental results of the Method (i)

Video #	# of cluster	All Frame									Period							
		Frame Num	AB	people	No people	TP	FN	FP	TN	Accuracy	Period Num	people	No People	TP	FN	FP	TN	Accuracy
1	4	61	10	46	5	43	3	0	8	94%	16	14	2	14	0	0	2	100%
2	4	71	6	57	8	38	19	0	8	71%	18	16	2	10	4	0	2	67%
3	3	50	0	44	6	43	1	0	6	98%	17	15	2	15	0	0	2	100%
4	4	75	4	66	5	61	5	0	5	93%	19	18	1	18	0	0	1	100%
5	4	59	0	55	4	47	8	0	4	86%	15	14	1	14	0	0	1	100%
6	4	79	1	73	5	61	12	0	5	85%	20	19	1	18	1	0	1	95%
7	3	53	0	44	9	25	19	0	9	64%	18	12	6	12	0	0	6	100%
8	2	37	0	35	2	30	5	0	2	86%	19	18	1	16	2	0	1	89%
9	4	47	0	43	4	40	3	0	4	94%	12	11	1	11	0	0	1	100%
10	2	29	1	25	3	23	2	0	3	93%	15	13	2	11	2	0	2	87%
11	4	135	0	106	29	88	13	0	29	87%	34	27	7	27	0	0	7	100%
12	5	274	29	218	30	181	37	12	30	85%	55	50	5	42	8	0	5	85%
13	5	109	6	75	28	63	2	10	28	88%	22	18	4	18	0	0	4	100%
14	5	84	1	72	11	67	1	4	11	94%	17	15	2	15	0	1	2	88%

ISBN: 978-988-18210-9-6
ISSN: 2078-0958 (Print); ISSN: 2078-0966 (Online)

Table 2. Experimental results of the Method (ii)

video#	All Frame								Period							
	Frame#	people	No people	TP	FN	FP	TN	Accuracy	Period#	People	No people	TP	FN	FP	TN	Accuracy
1	716	650	66	547	50	76	43	82%	40	36	4	33	2	4	3	90%
2	415	395	20	240	0	155	20	63%	28	26	2	17	0	9	2	68%
3	372	316	56	312	4	0	56	100%	57	52	5	52	0	0	5	100%
4	968	938	30	930	8	0	30	99%	61	59	2	57	2	0	2	97%
5	747	702	45	702	0	0	45	100%	47	44	3	44	0	0	3	100%
6	972	898	74	606	0	316	50	67%	75	70	5	66	0	6	4	93%
7	890	676	214	613	63	0	214	93%	56	44	12	39	5	0	2	91%
8	978	883	95	646	15	222	95	76%	61	55	6	42	1	12	6	79%
9	647	578	69	578	0	0	69	100%	64	58	6	58	0	0	6	100%
10	795	658	137	575	26	122	72	81%	56	51	5	40	2	9	5	80%
11	470	426	44	426	0	0	44	100%	30	27	3	27	0	0	3	100%
12	905	813	92	763	0	50	92	94%	58	54	4	52	0	2	4	97%
13	331	211	120	211	0	0	120	100%	23	15	8	15	0	0	8	100%
14	279	247	32	247	0	0	32	100%	17	15	2	15	0	0	2	100%

REFERENCES

[1] W.C. Teng, "A New Design of IR Illuminator for Nighttime Surveillance," *MS Thesis*, National Chiao Tung Univ., 2010.

[2] S. Mangiat and J. Gibson, "High Dynamic Range Video with Ghost Removal," *Society of Photo-Optical Instrumentation Engineers*, vol. 7798, pp. 30, 2010.

[3] S. B., Kang, M., Uyttendaele, S., Winder, and R., Szeliski, "High dynamic range video," *ACM Transactions on Graphics*, vol. 22, no. 3, 2003.

[4] S. Mangiat and J. D. Gibson, "Automatic Scene Relighting for Video Conferencing," *in Proc. IEEE Int'l Conf. Image Processing*, 2009.

[5] Y. Benezeth, B. Emile, H. Laurent and C. Rosenberger, "A Real Time Human Detection System Based on Far Infrared Vision," *in Proc. Image and Signal Processing*, 2008

[6] J. Ge, Y. Luo, and G. Tei, "Real-time pedestrian detection and tracking at nighttime for driver-assistance systems," *in Proc. IEEE Transactions on Intelligent Transportation Systems*, vol. 10, no. 2, pp. 283-298, 2009.

[7] Y. Fang, K. Yamada, Y. Ninomiya, B. Horn, and I. Masaki, "Comparison between infrared-image-based and visible-image-based approaches for pedestrian detection," *in Proc. IEEE Intelligent Vehicles Symposium*, 2003.

[8] M. Bertozzi, A. Broggi, A. Lasagni, and M. D. Rose, "Infrared stereo vision-based pedestrian detection," *in Proc. IEEE Intelligent Vehicles Symposium*, 2005.

[9] C., Dai, Y., Zheng, and X., Li, "Pedestrian Detection and Tracking in Infrared Imagery Using Shape and Appearance," *Computer Vision and Image Understanding*, vol.106, no. 2-3, pp. 288-299, 2007.

[10] F.L. Xu, X. Liu and K. Fujimura, "Pedestrian Detection and Tracking with Night Vision", *IEEE Transaction on Intelligent Transportation Systems*, vol.6, no. 1, pp. 63-71, 2005.

[11] H. Nanda and L. Davis, "Probabilistic template based pedestrian detection in infrared videos", *in Proc. IEEE Intelligent Vehicles Symposium*, 2002.

ISBN: 978-988-18210-9-6
ISSN: 2078-0958 (Print); ISSN: 2078-0966 (Online)